Sliding mode control of the prismatic-prismatic-revolute mobile robot with a flexible joint *

Hebertt Sira-Ramírez †
Centro de Investigación y Estudios Avanzados del IPN (CINVESTAV-IPN)
Departamento Ingeniería Eléctica, Sección de Mecatrónica
Avenida I.P.N. # 2508
Col. San Pedro Zacatenco, A.P. 14-740
07300 México D.F., México
email: hsira@mail.cinvestav.mx
Phone: 52-5-747-3800, x-6308 Fax: 52-5-747-3866

March 13, 2000

Abstract

A sliding mode controller is proposed for the regulation of the prismatic-prismatic-revolute (PPR) mobile robot equipped with an underactuated arm coupled to the robot main body by means of a flexible joint. The system, which happens to be differentially flat, can then be robustly controlled using a combination of the sliding mode control approach and exact tracking error linearization of prescribed off-line planned trajectories facilitated by the flatness property of the system.

Keywords: Sliding mode control, Differential flatness, Mobile robots.

*This research was supported by the Centro de Investigación y Estudios Avanzados del IPN, (CINVESTAV-IPN), Mexico, by the Consejo Nacional de Ciencia y Tecnología (CONACYT) under Research Grant 32681-A

†On leave of absence from the Departamento de Sistemas de Control of the Universidad de Los Andes

1 Introduction

A finite dimensional nonlinear multivariable system is said to be *differentially flat* if it is equivalent, by means of *endogenous* feedback to a linear controllable system in decoupled Brunovsky's form. *Flat outputs* are defined as a set of independent variables, whose cardinality equals that of the control input set, which completely parameterize the system state variables and control inputs. In other words, all system variables are *differential functions* of the flat outputs. This means that they are functions of the flat outputs and of a finite number of their time derivatives. Many nonlinear systems of practical interest turn out to be differentially flat and, hence, linearizable by means of *endogenous feedback*. Theoretical and application developments of *Differential flatness* can be found in the several articles by Prof. M. Fliess and his colleagues [3], [4], [5]. Flatness has also been extended to linear and nonlinear delay differential systems and to systems described by linear partial differential equations. Even though flatness can be advantageously combined with many nonlinear controller design techniques, like backstepping and passivity-based control (see, respectively, Martín *et al* [6] and Sira-Ramirez [9]), a flat system is more naturally controlled by means of exact linearization. However, exact linearization is based in exact cancellation of systems nonlinearities and these invariably depend on system parameters. Exact linearization is thus known to exhibit a lack of robustness with respect to parameter uncertainty and unmodelled external signals affecting the system behavior.

Sliding mode control, on the other hand, enjoys great popularity due to its simplicity and enhanced robustness with respect to unmodelled perturbation input signals and parameter uncertainty. The fundamental developments of this interesting controller design technique were mainly carried out in the former Soviet Union where a wealth of scientists contributed to its development during the years. We refer the reader to the book by Utkin [10] where fundamental developments and interesting application examples can be found.

In this article, a dynamic nonlinear multivariable sliding mode controller is proposed for the trajectory tracking error regulation of the Prismatic-Prismatic-Revolute (PPR) mobile robot equipped with an underactuated arm which is coupled to the robot main body by means of a flexible joint. The PPR robotic system, treated by Reyhanoglu *et al* in [7] from the viewpoint of non-integrable dynamic constraints, has been shown to be differentially flat, in an article by Sira-Ramírez [8], and therefore to be equivalent by means of dynamic state feedback to a set of decoupled controllable linear systems. Comparisons between the feedback performance obtained from the exact linearization approach and the passsivity-based control approach, were carried out for the PPR robot in a paper by Espinoza *et al* [2]. The flatness property and its intrinsic linearizing endogenous feedback option is here advantageously combined with sliding mode control for the robust feedback regulation of several prescribed maneuvers for the mobile PPR robot.

This article is organized as follows: Section 2 deals with the modeling aspects of the PPR robot from a Lagrangian viewpoint and the verification of the flatness property of the system. Section 3 develops a sliding mode controller in terms of general trajectory tracking tasks for the mobile robot. Section 4 is devoted to present simulation results and evaluates the robustness of the performance of the proposed controller for a typical maneuver. The last section presents the conclusions and suggestions for further research.

2 The PPR mathematical model and some of its properties

2.1 Derivation of the PPR robot model

Consider the PPR mobile robot, shown in Figure 1, with $\theta_2 = \theta + \phi$. We denote by (x, y) the vertical projection of the end effector position (of mass m) on the plane of coordinates, (X, Y), on which the robot main body (of mass M) translational motions take place. We refer, however, to (x, y) as the arm's tip coordinates. The geometric features of the system readily reveal the following set of relations between the

(x, y) coordinates and the main body center of gravity coordinates (x_b, y_b).

$$\begin{array}{lll} x = x_B + l\cos(\theta_2) & \Rightarrow & \dot{x} = \dot{x}_B - l\dot{\theta}_2 \sin(\theta_2) \\ y = y_B + l\sin(\theta_2) & & \dot{y} = \dot{y}_B + l\dot{\theta}_2 \cos(\theta_2) \end{array}$$

Within a Lagrangian dynamics viewpoint, we take as *generalized coordinates* the vector;

$$q = [x_B, y_B, \theta, \theta_2]^T$$

With reference to these coordinates, the kinetic energy function for the system, is given by

$$\mathcal{T}(\dot{x}_B, \dot{y}_B, \dot{x}, \dot{y}, \dot{\theta}) = \frac{1}{2}\left(M\dot{x}_B^2 + M\dot{y}_B^2 + m\dot{x}^2 + m\dot{y}^2 + I\dot{\theta}^2 \right)$$

This expression can also be written, more compactly, as $\mathcal{T}(q, \dot{q}) = \frac{1}{2}\dot{q}^T D(q)\dot{q}$, with

$$D(q) = \begin{bmatrix} M+m & 0 & 0 & -ml\sin(\theta_2) \\ 0 & M+m & 0 & ml\cos(\theta_2) \\ 0 & 0 & I & 0 \\ -ml\sin(\theta_2) & ml\cos(\theta_2) & 0 & ml^2 \end{bmatrix}$$

On the other hand, the torsion spring, assumed to be linear, is regarded as physically acting between the angular orientation of the body, θ, and that of the arm, θ_2. The potential energy is then given by

$$V(q) = \frac{1}{2}K(\theta - \theta_2)^2 = \frac{1}{2}q^T \mathcal{K} q$$

with

$$\mathcal{K} = \begin{bmatrix} 0 & 0 & 0 & 0 \\ 0 & 0 & 0 & 0 \\ 0 & 0 & K & -K \\ 0 & 0 & -K & K \end{bmatrix}$$

Thus, the Lagrangian of the system is obtained as,

$$\mathcal{L}(q, \dot{q}) = \frac{1}{2}\dot{q}^T D(q)\dot{q} - \frac{1}{2}q^T \mathcal{K} q$$

The vector of *generalized external forces* is seen to be

$$Q = [F_1, F_2, T, 0]^T$$

where F_1 and F_2 are the forces applied to the robot's main body center of gravity in order to achieve translational movement of the robot on the plane. T is the torque applied to the base revolute portion of the mechanical system, thus creating angular movement, through the flexible joint, of the robot's arm.

Applying the Euler-Lagrange equations, the model for the robot is seen to be of the following general form,

$$D(q)\ddot{q} + W(q, \dot{q}) + \mathcal{K}q = Q$$

where the term of Coriolis and centripetal forces,

$$W(q, \dot{q}) = \begin{bmatrix} -ml\dot{\theta}_2^2 \cos(\theta_2) \\ -ml\dot{\theta}_2^2 \sin(\theta_2) \\ 0 \\ 0 \end{bmatrix}$$

can be factored as

$$C(q,\dot{q}) = \begin{bmatrix} 0 & 0 & 0 & -ml\dot{\theta}_2\cos(\theta_2) \\ 0 & 0 & 0 & -ml\theta_2\dot{\theta}_2\sin(\theta_2) \\ 0 & 0 & 0 & 0 \\ 0 & 0 & 0 & 0 \end{bmatrix} \dot{q}$$

Note that the matrix $\overline{D}(q,\dot{q}) = \dot{D}(q) - 2C(q,\dot{q})$ is skew-symmetric. This property can be exploited in passivity-based regulation schemes of the PPR robot (see [2]).

The system is therefore characterized by the following implicit state space model

$$\begin{aligned} (M+m)\ddot{x}_B - ml\sin(\theta_2)\ddot{\theta}_2 - ml\dot{\theta}_2^2\cos(\theta_2) &= F_1 \\ (M+m)\ddot{y}_B + ml\cos(\theta_2)\ddot{\theta}_2 - ml\dot{\theta}_2^2\sin(\theta_2) &= F_2 \\ I\ddot{\theta} + K(\theta-\theta_2) &= T \\ ml^2\ddot{\theta}_2 - ml\sin(\theta_2)\ddot{x}_B + ml\cos(\theta_2)\ddot{y}_B - K(\theta-\theta_2) &= 0 \end{aligned} \tag{2.1}$$

2.2 Flatness property of the PPR robot model

The PPR robot model (2.1) is easily seen to be differentially flat. Indeed, the flat outputs are given by the main body center of gravity position coordinates, x_B, y_B, and the orientation angle, θ_2, of the robot arm. Indeed, all variables in the system (i.e. states and control inputs) are expressible as *differential functions* of the flat coordinates, (x_B, y_B, θ_2).

$$\begin{aligned} \theta &= \theta_2 + \frac{1}{K}\left[ml^2\ddot{\theta}_2 - ml\ddot{x}_B\sin(\theta_2) + ml\ddot{y}_B\cos(\theta_2)\right] \\ F_1 &= (M+m)\ddot{x}_B - ml\sin(\theta_2)\ddot{\theta}_2 - ml\dot{\theta}_2^2\cos(\theta_2) \\ F_2 &= (M+m)\ddot{y}_B + ml\cos(\theta_2)\ddot{\theta}_2 - ml\dot{\theta}_2^2\sin(\theta_2) \\ T &= -ml\ddot{x}_B\sin(\theta_2) + ml\ddot{y}_B\cos(\theta_2) + (I+ml^2)\ddot{\theta}_2 + \frac{I}{K}\Big[ml^2\theta_2^{(4)} \\ &\quad + ml\left(y_B^{(4)} - \dot{\theta}_2^2\ddot{y}_B - \ddot{\theta}_2\ddot{x}_B - 2\dot{\theta}_2 x_B^{(3)}\right)\cos(\theta_2) \\ &\quad - ml\left(x_B^{(4)} - \dot{\theta}_2^2\ddot{x}_B + \ddot{\theta}_2\ddot{y}_B + 2\dot{\theta}_2 y_B^{(3)}\right)\sin(\theta_2)\Big] \end{aligned} \tag{2.2}$$

Note that the end effector position is also expressible in terms of the flat outputs, by means of

$$x = x_B + l\cos(\theta_2), \quad y = y_B + l\sin(\theta_2)$$

The differential parameterization (2.2) allows one to compute explicitly off-line suitable reference trajectories for all state variables of the system in terms of desired flat output reference trajectories.

2.3 Invertibility of the differential parameterization

The structure of the dependence of the control inputs on the flat output time derivatives reveals that, while the torque control input T depends up to fourth order time derivatives of all the flat outputs, the forces F_1 and F_2 involve at most second order time derivatives of only two flat outputs. The multivariable input-flat output relation is, therefore, not an invertible one in the sense that the higher order derivatives of the flat outputs are not in a one to one relationship with a possible set of independent control inputs. A *dynamic extension* is therefore needed on the first two control inputs in order to achieve a desirable input-flat output "decoupling".

The required one-to-one relation would then read

$$\begin{aligned}
\ddot{F}_1 &= (m+M)x_B^{(4)} - ml\left[\theta_2^{(4)} - 6(\dot{\theta}_2)^2\ddot{\theta}_2\right]\sin(\theta_2) - ml\left[4\dot{\theta}_2\theta_2^{(3)} + 3(\ddot{\theta}_2)^2 - (\dot{\theta}_2)^4\right]\cos(\theta_2)\\
\ddot{F}_2 &= (m+M)y_B^{(4)} - ml\left[4\dot{\theta}_2\theta_2^{(3)} + 3(\ddot{\theta}_2)^2 - (\dot{\theta}_2)^4\right]\sin(\theta_2) + ml\left[\theta_2^{(4)} - 6(\dot{\theta}_2)^2\ddot{\theta}_2\right]\cos(\theta_2)\\
T &= (I+ml^2)\ddot{\theta}_2 + \frac{I}{K}\Big[ml^2\theta_2^{(4)} - ml\left(x_B^{(4)} + \left[\frac{K}{I} - \dot{\theta}_2^2\right]\ddot{x}_B + \ddot{\theta}_2\ddot{y}_B + 2\dot{\theta}_2 y_B^{(3)}\right)\sin(\theta_2)\\
&\quad + ml\left(y_B^{(4)} + \left[\frac{K}{I} - \dot{\theta}_2^2\right]\ddot{y}_B - \ddot{\theta}_2\ddot{x}_B - 2\dot{\theta}_2 x_B^{(3)}\right)\cos(\theta_2)\Big]
\end{aligned}$$

Considering $\ddot{F}_1$ and $\ddot{F}_2$ as new control inputs, we can rewrite the above relation as

$$\begin{bmatrix} m+M & 0 & -ml\sin(\theta_2) \\ 0 & m+M & ml\cos(\theta_2) \\ -ml\sin(\theta_2) & ml\cos(\theta_2) & ml^2 \end{bmatrix} \begin{bmatrix} x_B^{(4)} \\ y_B^{(4)} \\ \theta_2^{(4)} \end{bmatrix} =$$

$$\begin{bmatrix} -6ml(\dot{\theta}_2)^2\ddot{\theta}_2\sin(\theta_2) + ml\left[4\dot{\theta}_2\theta_2^{(3)} + 3(\ddot{\theta}_2)^2 - (\dot{\theta}_2)^4\right]\cos(\theta_2) + \ddot{F}_1 \\ ml\left[4\dot{\theta}_2\theta_2^{(3)} + 3(\ddot{\theta}_2)^2 - (\dot{\theta}_2)^4\right]\sin(\theta_2) + 6ml(\dot{\theta}_2)^2\ddot{\theta}_2\cos(\theta_2) + \ddot{F}_2 \\ \Big\{ -\frac{K}{I}(I+ml^2)\ddot{\theta}_2 + ml\left(\left[\frac{K}{I} - \dot{\theta}_2^2\right]\ddot{x}_B + \ddot{\theta}_2\ddot{y}_B + 2\dot{\theta}_2 y_B^{(3)}\right)\sin(\theta_2) \\ \qquad -ml\left(\left[\frac{K}{I} - \dot{\theta}_2^2\right]\ddot{y}_B - \ddot{\theta}_2\ddot{x}_B - 2\dot{\theta}_2 x_B^{(3)}\right)\cos(\theta_2) + \frac{K}{I}T\Big\} \end{bmatrix}$$

The global invertibility of the matrix in the left hand side of the previous expression implies that a suitable (global) state-dependent input coordinate transformation reduces the system to the following decoupled set of linear controllable systems in Brunovsky's canonical form,

$$x_B^{(4)} = v_1, \quad y_B^{(4)} = v_2, \quad \theta_2^{(4)} = v_3 \tag{2.3}$$

with v_1, v_2 and v_3 defined in the obvious way.

2.4 Control objectives

It is desired primarily to execute a feedback controlled translational motion of the PPR robot, along with some requirements on the arm orientation. Generally we would have available a specification of the nominal motions as a set of functions: $x_B^*(t)$, $y_B^*(t)$ and $\theta_2^*(t)$ characterizing, respectively, the desired main body movement and the desired orientation of the arm. In some other examples, it is desired to follow a particular trajectory characterized by a prescribed body movement and the body orientation; $x_B^*(t)$, $y_B^*(t)$ and $\theta^*(t)$, while, as in [7], it is additionally required that the robot's arm actual angular position, θ_2, evolves at the nominal value of zero during the execution of the trajectory tracking maneuver. In this last kind of maneuvers it is implied that no vibrations are allowed which are due to revolute joint flexibility during the maneuver. It is clear, from the flatness property, that any desired maneuver, regardless of its particular specifications, can always be translated to a required nominal maneuver, exclusively given in terms of suitable trajectories for the flat outputs. For this reason, we concentrate our controller design efforts in achieving asymptotic trajectory tracking for the flat output coordinates (x_B, y_B, θ_2).

3 Sliding mode feedback controller design

3.1 An exact tracking error linearization approach

Consider the following discrete sets of real constant coefficients,

$$\{\beta_{0x},\beta_{1x},\beta_{2x},\beta_{3x}\},\quad \{\beta_{0y},\beta_{1y},\beta_{2y},\beta_{3y}\},\quad \{\beta_{0\theta_2},\beta_{1\theta_2},\beta_{2\theta_2},\beta_{3\theta_2}\}$$

Assume that each particular described set constitutes a *Hurwitz set.* In other words, they are associated with *stable* polynomials, defined in terms of the complex variable λ, which are of the following form

$$p_{(\cdot)}(\lambda) = \lambda^4 + \beta_{3(\cdot)}\lambda^3 + \beta_{2(\cdot)}\lambda^2 + \beta_{1(\cdot)}\lambda + \beta_{0(\cdot)}$$

We denote by $p_{(\cdot)}(\frac{d}{dt})$ the associated differential polynomial,

$$p_{(\cdot)}(\frac{d}{dt}) = \frac{d^4}{dt^4} + \beta_{3(\cdot)}\frac{d^3}{dt^3} + \beta_{2(\cdot)}\frac{d^2}{dt^2} + \beta_{1(\cdot)}\frac{d}{dt} + \beta_{0(\cdot)}$$

Proposition 3.1 *Given a prescribed trajectory, $\{x_B^*(t), y_B^*(t), \theta_2^*(t)\}$ for the flat outputs of the PPR robot (2.1), the following* dynamic *feedback controller, achieves closed-loop asymptotic exponential tracking of the given path.*

$$\begin{aligned}
\ddot{F}_1 &= (m+M)v_x - ml\left[v_{\theta_2} - 6(\dot{\theta}_2)^2\ddot{\theta}_2\right]\sin(\theta_2) - ml\left[4\dot{\theta}_2\theta_2^{(3)} + 3(\ddot{\theta}_2)^2 - (\dot{\theta}_2)^4\right]\cos(\theta_2)\\
\ddot{F}_2 &= (m+M)v_y - ml\left[4\dot{\theta}_2\theta_2^{(3)} + 3(\ddot{\theta}_2)^2 - (\dot{\theta}_2)^4\right]\sin(\theta_2) + ml\left[v_{\theta_2} - 6(\dot{\theta}_2)^2\ddot{\theta}_2\right]\cos(\theta_2)\\
T &= (I+ml^2)\ddot{\theta}_2 + \frac{I}{K}\left[ml^2 v_{\theta_2} - ml\left(v_x + \left[\frac{K}{I} - \dot{\theta}_2^2\right]\ddot{x}_B + \ddot{\theta}_2\ddot{y}_B + 2\dot{\theta}_2 y_B^{(3)}\right)\sin(\theta_2)\right.\\
&\quad \left. + ml\left(v_y + \left[\frac{K}{I} - \dot{\theta}_2^2\right]\ddot{y}_B - \ddot{\theta}_2\ddot{x}_B - 2\dot{\theta}_2 x_B^{(3)}\right)\cos(\theta_2)\right]
\end{aligned}$$

with

$$\begin{aligned}
v_x &= \frac{d^4}{dt^4}x_B^*(t) - \beta_{3x}(x_B^{(3)} - \frac{d^3}{dt^3}x_B^*(t)) - \beta_{2x}(\ddot{x}_B - \frac{d^2}{dt^2}x_B^*(t)) - \beta_{1x}(\dot{x}_B - \frac{d}{dt}x_B^*(t)) - \beta_{0x}(x_B - x_B^*(t))\\
v_y &= \frac{d^4}{dt^4}y_B^*(t) - \beta_{3y}(y_B^{(3)} - \frac{d^3}{dt^3}y_B^*(t)) - \beta_{2y}(\ddot{y}_B - \frac{d^2}{dt^2}y_B^*(t)) - \beta_{1y}(\dot{y}_B - \frac{d}{dt}y_B^*(t)) - \beta_{0y}(y_B - y_B^*(t))\\
v_{\theta_2} &= \frac{d^4}{dt^4}\theta_2{}^*(t) - \beta_{3\theta_2}(\theta_2{}^{(3)} - \frac{d^3}{dt^3}\theta_2{}^*(t)) - \beta_{2\theta_2}(\ddot{\theta}_2 - \frac{d^2}{dt^2}\theta_2{}^*(t)) - \beta_{1\theta_2}(\dot{\theta}_2 - \frac{d}{dt}\theta_2{}^*(t)) - \beta_{0\theta_2}(\theta_2 - \theta_2{}^*(t))
\end{aligned}$$

Proof

Let e_x, e_y and e_{θ_2} denote, respectively, the tracking errors, $x_B - x_B^*(t)$, $y_B - y_B^*(t)$ and $\theta_2 - \theta_2{}^*(t)$. The proposed controller yields the following closed-loop tracking error dynamics

$$\begin{bmatrix} M+m & 0 & -ml\sin(\theta_2) \\ 0 & M+m & ml\cos(\theta_2) \\ -ml\sin(\theta_2) & ml\cos(\theta_2) & ml^2 \end{bmatrix} \begin{bmatrix} [p_x(\frac{d}{dt})]\, e_x \\ [p_y(\frac{d}{dt})]\, e_y \\ [p_{\theta_2}(\frac{d}{dt})]\, e_{\theta_2} \end{bmatrix} = 0$$

Since the above matrix is non-singular, it follows that

$$\left[p_x(\frac{d}{dt})\right] e_x = 0,\quad \left[p_y(\frac{d}{dt})\right] e_y = 0,\quad \left[p_{\theta_2}(\frac{d}{dt})\right] e_{\theta_2} = 0$$

and therefore e_x, e_y and e_{θ_2} asymptotically exponentially converge to zero.

□

The linearizing controller derived above is based on exact cancellation of the system's non-linearities. The performance of the linearizing controller deteriorates when unmodelled external perturbation inputs and uncertain parameter perturbations affect the system. In the next section we still propose to take advantage of the simplicity of a linearizing controller but this time endowed with robustness features borrowed from sliding mode control.

3.2 A property of sliding mode control

Let σ be a scalar quantity and W be strictly positive constant. Suppose $\xi(t)$ is an unknown perturbation signal with uniformly bounded magnitude for all $t \geq 0$, i.e.

$$\max_{t \geq 0} |\xi(t)| \leq B$$

The following proposition is a standard result in sliding mode control (see Utkin [10]).

Proposition 3.2 *Given any arbitrary initial value $\sigma(0)$ of σ, the closed-loop trajectories, $\sigma(t)$, of the discontinous perturbed dynamics,*

$$\dot{\sigma} = -W \operatorname{sign} \sigma + \xi(t)$$

converge to zero, in finite time, T, if and only if $W > B$. Moreover, T is upper bounded by the quantity

$$\frac{|\sigma(0)|}{W - B}$$

□

The sliding mode trajectories of the scalar function σ are, therefore, *robust* with respect to unmodelled additive bounded perturbation input signals. Our results below are based on this fundamental fact.

3.3 A property of high-gain control

A widely recognized disadvantage of sliding mode controllers is the, so-called, "chattering phenomenon" by which the high frequency "bang-bang" control input excites unmodelled parasitic dynamics and causes oscillatory motions in the system's directly actuated variables, thus degrading the closed-loop performance. A popular technique, which still has fast stabilizing features but which lacks the degree of robustness of sliding mode control, consists of replacing the discontinuous controller by a high gain controller. The following result establishes the salient features of such substitution in fundamental terms.

Proposition 3.3 *Given any arbitrary initial value $\sigma(0)$ of the scalar quantity, σ, the closed-loop trajectories, $\sigma(t)$, of the "high-gain" controlled perturbed dynamics,*

$$\dot{\sigma} = -W \frac{\sigma}{|\sigma| + \epsilon} + \xi(t)$$

crosses, in finite time T, the boundary of a neighborhood of zero, of radius R, from whose interior the trajectory never escapes, if and only if $W > B$. Moreover, T and R satisfy

$$T \leq \frac{|\sigma(0)|}{W - B}, \quad R = \frac{\epsilon}{W/B - 1}$$

Proof

Consider the Lyapunov function candidate $V(\sigma) = \frac{1}{2}\sigma^2$. The time derivatives of $V(\sigma)$ along the closed-loop perturbed trajectories of $\sigma(t)$ satisfy,

$$\begin{aligned} \dot{V}(\sigma) &= \sigma\dot{\sigma} = -W\left(\frac{\sigma^2}{|\sigma|+\epsilon}\right) + \sigma\xi(t) \leq -W\left(\frac{|\sigma|^2}{|\sigma|+\epsilon}\right) + |\sigma||\xi(t)| \\ &= -|\sigma|\left[W\left(\frac{|\sigma|}{|\sigma|+\epsilon}\right) - B\right] = -\left(\frac{|\sigma|}{|\sigma|+\epsilon}\right)\left[|\sigma|(W-B) - B\epsilon\right] \end{aligned} \tag{3.1}$$

Thus $\dot{V}$ is negative everywhere except in the interior of the ball given by

$$\mathcal{B} = \{\sigma : |\sigma| \leq \frac{B\epsilon}{W-B}\}$$

thus the trajectories of σ approach $\mathcal{B}$ from the outside, and are constrained by $\mathcal{B}$ when they start from the inside. Note that the boundary of the ball $\mathcal{B}$, does not contain system trajectories since, on the boundary the closed-loop system satisfies: $\dot{\sigma} = -B\text{sign}\ \sigma + \xi(t)$ and $\sigma\dot{\sigma} = -|\sigma|(B - \xi(t)\text{sign}\ \sigma) < 0$. The boundary of $\mathcal{B}$ is not an *invariant set*. Hence, any trajectory starting outside $\mathcal{B}$ crosses its boundary and, thus, $\mathcal{B}$ is reachable in finite time. Integrating the differential equation for σ and uniformly upper bounding $|\xi(t)|$ by B and the quantity, $|\sigma(t)|/(|\sigma(t)| + \epsilon)$, by 1, yields the time estimate T.

□

3.4 Dynamic sliding mode control of the PPR mobile robot

Consider the following sets of constant coefficients,

$$\{\alpha_{0x}, \alpha_{1x}, \alpha_{2x}\}, \quad \{\alpha_{0y}, \alpha_{1y}, \alpha_{2y}\}, \quad \{\alpha_{0\theta_2}, \alpha_{1\theta_2}, \alpha_{2\theta_2}\}$$

As before, we assume that each set constitutes a *Hurwitz set*, i.e. they build *stable* polynomials of the following form,

$$p_{(\cdot)}(\lambda) = \lambda^3 + \alpha_{2(\cdot)}\lambda^2 + \alpha_{1(\cdot)}\lambda^1 + \alpha_{0(\cdot)}$$

We denote by $p_{(\cdot)}(\frac{d}{dt})$ the associated differential polynomial,

$$p_{(\cdot)}(\frac{d}{dt}) = \frac{d^3}{dt^3} + \alpha_{2(\cdot)}\frac{d^2}{dt^2} + \alpha_{1(\cdot)}\frac{d}{dt} + \alpha_{0(\cdot)}$$

Define, as before, the set of tracking errors $e_x = x_B - x^*(t)$, $e_y = y_B - y_B^*(t)$ and $e_{\theta_2} = \theta_2 - \theta_2^*(t)$.

Consider a set of sliding surfaces σ_x, σ_y and σ_{θ_2}, comprising a *sliding surface* vector, given by expressions of the form

$$\sigma_{(\cdot)} = \left[p_{(\cdot)}(\frac{d}{dt})\right] e_{(\cdot)}$$

Note that if the sliding vector components σ_x, σ_y and σ_{θ_2} are indefinitely constrained to be zero, by means of a control action, the corresponding tracking errors e_x, e_y and e_θ asymptotically exponentially converge to zero.

Proposition 3.4 *Given a desired nominal trajectory $\{x_B^*(t), y_B^*(t), \theta_2^*(t)\}$ for the flat outputs of the robot (2.1), the following* dynamic *sliding mode feedback controller, achieves asymptotic exponential tracking of the given path.*

$$
\begin{aligned}
\ddot{F}_1 &= (m+M)v_x - ml\left[v_{\theta_2} - 6(\dot{\theta}_2)^2\ddot{\theta}_2\right]\sin(\theta_2) - ml\left[4\dot{\theta}_2\theta_2^{(3)} + 3(\ddot{\theta}_2)^2 - (\dot{\theta}_2)^4\right]\cos(\theta_2) \\
\ddot{F}_2 &= (m+M)v_y - ml\left[4\dot{\theta}_2\theta_2^{(3)} + 3(\ddot{\theta}_2)^2 - (\dot{\theta}_2)^4\right]\sin(\theta_2) + ml\left[v_{\theta_2} - 6(\dot{\theta}_2)^2\ddot{\theta}_2\right]\cos(\theta_2) \\
T &= (I+ml^2)\ddot{\theta}_2 + \frac{I}{K}\left[ml^2 v_{\theta_2} - ml\left(v_x + \left[\frac{K}{I} - \dot{\theta}_2^2\right]\ddot{x}_B + \ddot{\theta}_2\ddot{y}_B + 2\dot{\theta}_2 y_B^{(3)}\right)\sin(\theta_2)\right. \\
&\quad \left. + ml\left(v_y + \left[\frac{K}{I} - \dot{\theta}_2^2\right]\ddot{y}_B - \ddot{\theta}_2\ddot{x}_B - 2\dot{\theta}_2 x_B^{(3)}\right)\cos(\theta_2)\right]
\end{aligned} \tag{3.2}
$$

with

$$
\begin{aligned}
v_x &= \frac{d^4}{dt^4}x_B^*(t) - \alpha_{2x}(x_B^{(3)} - \frac{d^3}{dt^3}x_B^*(t)) - \alpha_{1x}(\ddot{x}_B - \frac{d^2}{dt^2}x_B^*(t)) - \alpha_{0x}(\dot{x}_B - \frac{d}{dt}x_B^*(t)) - W_x \text{ sign } \sigma_x \\
v_y &= \frac{d^4}{dt^4}y_B^*(t) - \alpha_{2y}(y_B^{(3)} - \frac{d^3}{dt^3}y_B^*(t)) - \alpha_{1y}(\ddot{y}_B - \frac{d^2}{dt^2}y_B^*(t)) - \alpha_{0y}(\dot{y}_B - \frac{d}{dt}y_B^*(t)) - W_y \text{ sign } \sigma_y \\
v_{\theta_2} &= \frac{d^4}{dt^4}\theta_2{}^*(t) - \alpha_{2\theta_2}(\theta_2{}^{(3)} - \frac{d^3}{dt^3}\theta_2{}^*(t)) - \alpha_{1\theta_2}(\ddot{\theta}_2 - \frac{d^2}{dt^2}\theta_2{}^*(t)) - \alpha_{0\theta_2}(\dot{\theta}_2 - \frac{d}{dt}\theta_2{}^*(t)) - W_{\theta_2} \text{ sign } \sigma_{\theta_2}
\end{aligned} \tag{3.3}
$$

where W_x, W_y and W_{θ_2} are, sufficiently large, strictly positive constants and the function "sign" stands for the signum *function.*

Proof

The proposed dynamic discontinuous feedback controller yields the following closed-loop sliding surface vector dynamics

$$
\begin{bmatrix} M+m & 0 & -ml\sin(\theta_2) \\ 0 & M+m & ml\cos(\theta_2) \\ -ml\sin(\theta_2) & ml\cos(\theta_2) & ml^2 \end{bmatrix}
\begin{bmatrix} \frac{d}{dt}\left\{\left[p_x(\frac{d}{dt})\right]e_x\right\} + W_x \text{ sign } \sigma_x \\ \frac{d}{dt}\left\{\left[p_y(\frac{d}{dt})\right]e_x\right\} + W_y \text{ sign } \sigma_y \\ \frac{d}{dt}\left\{\left[p_{\theta_2}(\frac{d}{dt})\right]e_{\theta_2}\right\} + W_{\theta_2} \text{ sign } \sigma_{\theta_2} \end{bmatrix} = 0
$$

i.e.

$$
\begin{bmatrix} M+m & 0 & -ml\sin(\theta_2) \\ 0 & M+m & ml\cos(\theta_2) \\ -ml\sin(\theta_2) & ml\cos(\theta_2) & ml^2 \end{bmatrix}
\begin{bmatrix} \frac{d}{dt}\sigma_x + W_x \text{ sign } \sigma_x \\ \frac{d}{dt}\sigma_y + W_y \text{ sign } \sigma_y \\ \frac{d}{dt}\sigma_{\theta_2} + W_{\theta_2} \text{ sign } \sigma_{\theta_2} \end{bmatrix} = 0
$$

It follows that

$$
\frac{d}{dt}\sigma_x + W_x \text{ sign } \sigma_x = 0, \quad \frac{d}{dt}\sigma_y + W_y \text{ sign } \sigma_y = 0, \quad \frac{d}{dt}\sigma_{\theta_2} + W_{\theta_2} \text{ sign } \sigma_{\theta_2} = 0
$$

and therefore σ_x, σ_y and σ_{θ_2} converge to zero in *finite time*. As a consequence, the tracking errors e_x, e_y and e_{θ_2} asymptotically exponentially converge to zero.

□

4 Simulation results

We considered a mobile PPR robot with the following physical parameters:

$$
m = 3 \text{ Kg}, \quad M = 10 \text{ Kg}, \quad k = 0.5 \text{ N} - \text{m/rad}, \quad J = 0.1 \text{ N} - \text{m} - \text{s}^2/\text{rad}, \quad l = 0.5 \text{ m}
$$

We tested the performance of the dynamic sliding mode controller (3.2), (3.3), for the tracking of a planned nominal trajectories of the flat output variables, $(x_B^*(t), y_B^*(t), \theta_2^*(t))$.

4.1 Tracking a circular trajectory (arm aiming at a fixed point)

A circular path of radius R was specified for the main body center of mass coordinates (x_B, y_B). The corresponding circle defined in the plane (X, Y) with center located on the Y axis, at the point $(0, R)$,

$$x_B^*(t) = R\sin(\omega t), \quad y_B^*(t) = R(1-\cos(\omega t)), \quad R = 2 \text{ m}, \quad \omega = 0.1 \text{ rad/s}$$

It was desired to track the circular path while the robot arm was required to aim, at all times, inwards the circle, directly pointing towards the fixed point $(0, R)$ in the plane (X, Y). This demand implied that the nominal arm angular orientation, θ_2, had to satisfy, $\theta_2 = \omega t + \pi/2$. The nominal value of the body orientation angle, θ, computed, according to the first equation in (2.2), turns out to be,

$$\theta = \omega t + \frac{\pi}{2} - \frac{ml}{K}\left[\ddot{x}_B cos(\omega t) + \ddot{y}_B \sin(\omega t)\right] = \omega t + \frac{\pi}{2} \tag{4.1}$$

i.e., the body orientation angle θ coincides with the arm orientation angle θ_2. The torsion spring, thus, exercises no restoring torque along the nominal path.

In order to avoid chattering and undesired oscillations we proceeded to change the hard switch in the sliding mode controller by a high gain "soft" switch.

Simulation results, illustrating the robot change in position and the arm position, with initial conditions starting significantly off the planned trajectory, are given in Figure 2. The sliding mode controller parameters including the high gain switch parameters were set to be $W_x = W_y = 2, W_{\theta_2} = 1, \epsilon = 0.05$, while the sliding surfaces defining polynomials were chosen to be of the form:

$$\lambda^3 + (2\xi\omega_n + a)\lambda^2 + (2\xi\omega_n a + \omega_n^2)\lambda + \omega_n^2 a = (\lambda^2 + 2\xi\omega_n\lambda + \omega_n^2)(\lambda + a)$$

i.e., we specified the tracking errors linearized closed-loop dynamics by a characteristic polynomial with one real and two complex eigenvalues located in the left portion of the complex plane. We chose: $a = 2, \xi = 0.8, \omega_n = 1$ for the main body positions closed-loop dynamics, and $a = 1, \xi = 0.8, \omega_n = 1$ for the arm angular orientation closed-loop dynamics.

Figure 2 shows the time evolutions of the system generalized variables $x_B, y_B, \theta, \theta_2$ compared with their nominal trajectories $x_B^*(t), y_B^*(t), \theta^*(t), \theta_2^*(t)$. In this figure we also show the three control inputs. Figure 3 depicts the motions of the main body and of the end effector in the plane. The control system successfully tracks the prescribed trajectory.

A robustness test was also carried out to check for the effect of unmodelled sustained oscillatory perturbations which were also allowed to directly act on the underactuated arm position dynamics. For these simulations we used the following perturbed model of the PPR robot,

$$\begin{aligned}
(M+m)\ddot{x}_B - ml\sin(\theta_2)\ddot{\theta}_2 - ml\dot{\theta}_2^2\cos(\theta_2) &= F_1 \\
(M+m)\ddot{y}_B + ml\cos(\theta_2)\ddot{\theta}_2 - ml\dot{\theta}_2^2\sin(\theta_2) &= F_2 + 0.5\,\eta(t) \\
I\ddot{\theta} + K(\theta - \theta_2) &= T \\
ml^2\ddot{\theta}_2 - ml\sin(\theta_2)\ddot{x}_B + ml\cos(\theta_2)\ddot{y}_B - K(\theta - \theta_2) &= 0.1\,\eta(t)
\end{aligned} \tag{4.2}$$

with $\eta(t) = \sin(t)$.

Figure 4 shows the perturbed evolutions of the system generalized position variables $x_B, y_B, \theta, \theta_2$ compared with their nominal trajectories $x_B^*(t), y_B^*(t), \theta^*(t), \theta_2^*(t)$. The three control inputs are shown to absorb the unmodelled oscillatory perturbation in a quite efficient manner. The actuated body position coordinates are practically unaffected by the unmodelled perturbation while the controller still manages to reasonable regulate the unactuated coordinate, θ_2, towards the prescribed trajectory with small oscillations (see Figure 5).

4.2 Tracking a circular trajectory (arm aiming tangentially to the path)

It was also desired to track the same circular path specified above while the robot arm was required to aim, at all times, tangentially to the traversed circle defined in the plane (X, Y). The nominal arm angular orientation, θ_2, satisfied, then, $\theta_2 = \omega t$. The nominal value of the body orientation angle, θ, computed, according to the first equation in (2.2), turns out to be,

$$\theta = \omega t + \frac{\pi}{2} - \frac{ml}{K}\left[\ddot{x}_B cos(\omega t) + \ddot{y}_B \sin(\omega t)\right] = \omega t + \frac{mlR\omega^2}{K} \tag{4.3}$$

i.e., the body orientation angle θ has a constant offset with respect to the arm orientation angle θ_2 thus creating, on the torsion spring modeling the flexible joint, a constant restoring torque of value $mlR\omega^2$. The numerical values given yield a constant torque of 0.03 [N-m] with a constant offset of 0.06 [rad].

Figures 6 and 7 depict the evolution of the unperturbed motions of the mobile robot with the prescribed maneuver.

4.3 Point to point regulation along a straight line segment

Consider the motion represented by a straight line segment with prescribed initial point given by the coordinates, (x_{B0}, y_{B0}), and terminal point given by, (x_{Bf}, y_{Bf}) in the (X, Y) plane. The robot starts with zero velocity and arbitrary orientation off the line segment. While aligning the arm, it is required to reach the starting point of the line segment (x_{B0}, y_{B0}) and park there, then to proceed to follow the prescribed line segment during a finite period of time $[t_i, t_f]$ and, finally, park again at the specified final point (x_{Bf}, y_{Bf}). It is further required to execute a pointing maneuver of the arm which takes it along the same direction of the robot orientation angle coinciding with that of the prescribed line path.

For the desired maneuver we prescribe off-line a polynomial spline of the Bézier type for each of the flat output coordinates, $x_B^*(t)$, $y_B^*(t)$, and $\theta_2^*(t)$. The orientation angular trajectory,$\theta_2^*(t)$, has a different time interval specification than that of the translational variables trajectories $x_B^*(t)$, $y_B^*(t)$.

The nominal displacement and orientation variables were specified as

$$x_B^*(t) = x_{B0} + (x_{Bf} - x_{B0})\left(\frac{t-t_i}{t_f-t_i}\right)^5\left[r_1 - r_2\left(\frac{t-t_i}{t_f-t_i}\right) + r_3\left(\frac{t-t_i}{t_f-t_i}\right)^2 - \ldots - r_6\left(\frac{t-t_i}{t_f-t_i}\right)^5\right]$$

$$y_B^*(t) = y_{B0} + (y_{Bf} - y_{B0})\left(\frac{t-t_i}{t_f-t_i}\right)^5\left[r_1 - r_2\left(\frac{t-t_i}{t_f-t_i}\right) + r_3\left(\frac{t-t_i}{t_f-t_i}\right)^2 - \ldots - r_6\left(\frac{t-t_i}{t_f-t_i}\right)^5\right]$$

$$\theta_2^*(t) = \theta_{20} + (\theta_{2f} - \theta_{20})\left(\frac{t-t_{i\theta_2}}{t_{f\theta_2}-t_{i\theta_2}}\right)^5\left[r_1 - r_2\left(\frac{t-t_{i\theta_2}}{t_{f\theta_2}-t_{i\theta_2}}\right) + r_3\left(\frac{t-t_{i\theta_2}}{t_{f\theta_2}-t_{i\theta_2}}\right)^2 - \ldots - r_6\left(\frac{t-t_{i\theta_2}}{t_{f\theta_2}-t_{i\theta_2}}\right)^5\right]$$

We chose a nominal trajectory for the angular orientation θ_2 which tried to orient the arm from the beginning of the maneuver in a period of time $[t_{i\theta_2}, t_{f\theta_2}]$ which preceded the transfer maneuver interval $[t_i, t_f]$. The desired nominal body and arm orientation angles are the same as that of the line $\arctan[(y_{Bf} - y_{B0})/(x_{Bf} - x_{B0})] = \pi/4$ [rad].

The polynomial coefficients were chosen to be:

$$r_1 = 252,\ r_2 = 1050,\ r_3 = 1800,\ r_4 = 1575,\ r_5 = 700,\ r_6 = 126$$

and $t_i = 10$ [s], $t_f = 25$ [s], $t_{i\theta_2} = 0$, $t_{f\theta_2} = 10$, $(x_{Bf}, y_{Bf}) = (8.5, 8.5)$, $(x_{B0}, y_{B0}) = (0.5, 0.5)$

Figures 8 and 9 depict computer simulations illustrating the performance of the previously designed feedback controller for significant initial deviations from the prescribed path and from the prescribed orientation angle for both the robot body and the unactuated arm. These initial conditions, at time $t = t_0$, were set to be

$$x_B(t_0) = 2.0 \text{ [m]}\ \ y_B(t_0) = 3.0 \text{ [m]}\ \ \theta_2(t_0) = \pi \text{ [rad]}\ \ \theta(t_0) = \pi \text{ [rad]}$$

5 Conclusions

A dynamic sliding mode controller has been developed for the PPR mobile robotic with a flexible appendage. The proposed controller design method heavily relies in the differential flatness of the system, which is quite helpful in facilitating the off-line trajectory planning aspects which achieve a desired motion maneuver in the plane. To avoid the classical chattering behavior of sliding mode controlled mechanical systems, we carried out the implementation of the derived controller with the aid of a high gain saturation function replacing the troublesome switch. The simulation results show that the dynamic high gain controller practically retains all the nice qualitative characteristics of sliding mode control. Reasonable tracking accuracy and unmodelled perturbation rejection features were also present in the high gain controller.

References

[1] J. Baillieul, " Kinematically redundant robots with flexible components", *IEEE Contr. Syst. Mag.*, Vol. 13, pp. 15-21, 1993.

[2] G. Espinoza-Pérez, H. Sira-Ramírez and M. Rios-Bolívar, "Regulation of the Prismatic-Prismatic-Revolute Robot with a Flexible Joint: A combined passivity and flatness approach" (submitted for publication).

[3] M. Fliess, J. Lévine, Ph. Martín and P. Rouchon, "Sur les systèmes nonlinéaires différentiellement plats", C. R. Acad. Sci. Paris, I-315, pp. 619-624, 1992.

[4] M. Fliess, J. Lévine, Ph. Martín and P. Rouchon, "Flatness and defect of nonlinear systems: Introductory theory and examples ", *International Journal of Control*, Vol. 61 , pp. 1327-1361, 1995.

[5] M. Fliess, J. Lévine, Ph. Martín and P. Rouchon, " A Lie-Bäcklund approach to equivalence and flatness" *IEEE Transactions on Automatic Control*, Vol. 44, No. 5, pp. 922-937, May 1999.

[6] P. Martín, R. M. Murray, and P. Rouchon, " Flat systems", *Proc. of the 4th European Control Conference*, pp. 211-264, 1997.

[7] M. Reyhanoglu, A. van der Schaft and N. H. McCalmroch, " Dynamics and Control of a Class of Underactuated Mechanical Systems"*IEEE Transactions on Automatic Control*, Vol. AC-44, No. 9, September 1999.

[8] H. Sira-Ramírez, " Control of a PPR Robot with a Flexible Arm" (submitted for publication)

[9] H. Sira-Ramírez, " Passivity vs flatness in the regulation of an exothermic chemical reactor", *European Journal of Control*, Vol. 6, No. 3, 2000 (to appear).

[10] V. Utkin, "Sliding Motions in the Theory of Variable Structure Systems," MIR Publishers, Moscow, 1978.

LIST OF FIGURES

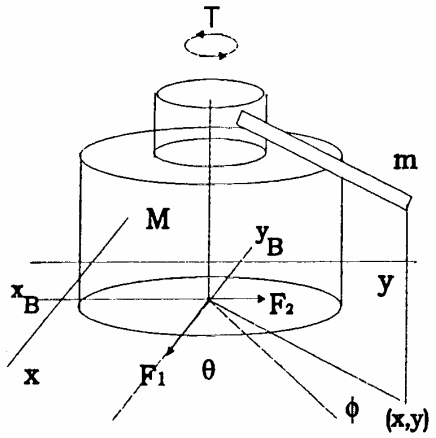

Figure 1: The PPR mobile robot.

Figure 4: State variables, end effector position and control inputs responses for perturbed circle tracking maneuver.

Figure 5: Circle tracking maneuver, main body and end effector perturbed position trajectories.

Figure 6: State variables, end effector position and control inputs responses for circle tracking maneuver with tangential arm pointing.

Figure 7: Circle tracking maneuver, main body and end effector position trajectories with tangential arm pointing.

Figure 8: State variables, end effector position and control inputs responses for a rest to rest maneuver in a line segment.

Figure 9: Portion of the line segment tracking maneuver: Main body and end effector position trajectories.

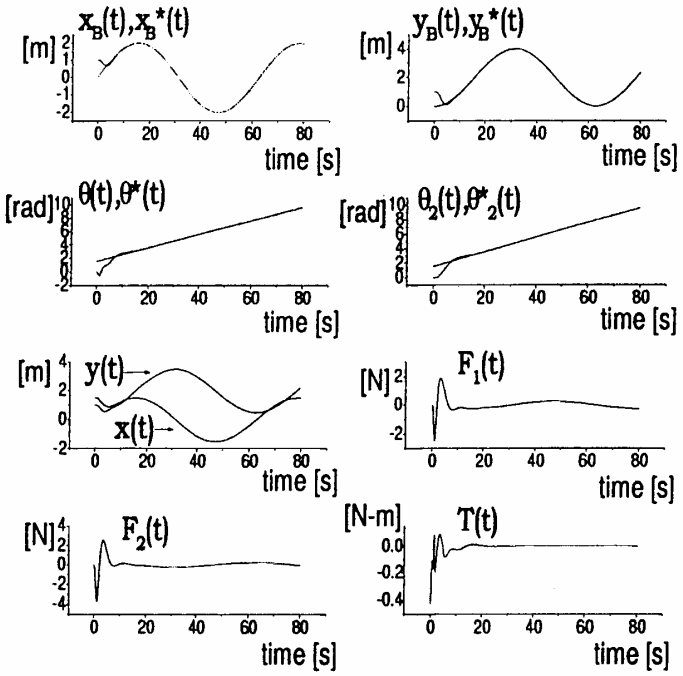

Figure 2: State variables, end effector position and control inputs responses for circle tracking maneuver.

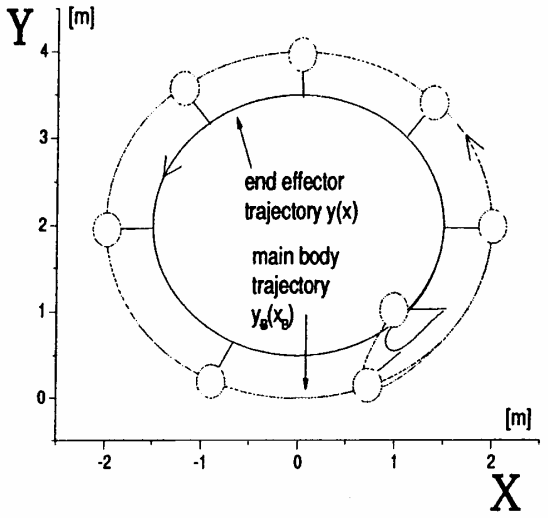

Figure 3: Circle tracking maneuver, main body and end effector position trajectories.

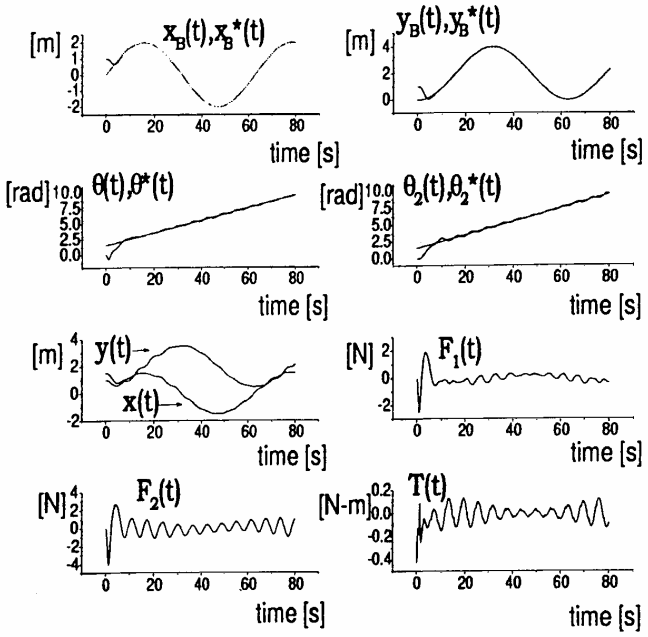

Figure 4: State variables, end effector position and control inputs responses for perturbed circle tracking maneuver.

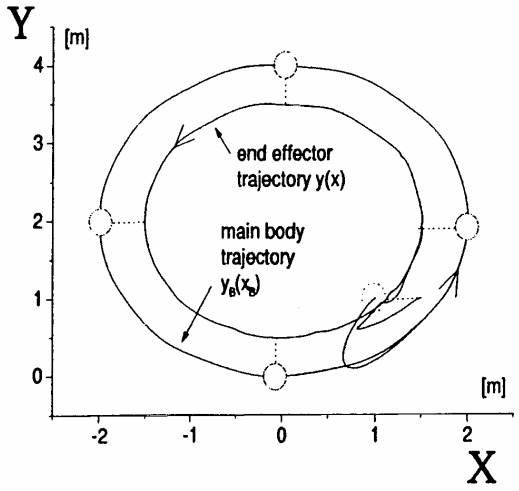

Figure 5: Circle tracking maneuver, main body and end effector perturbed position trajectories.

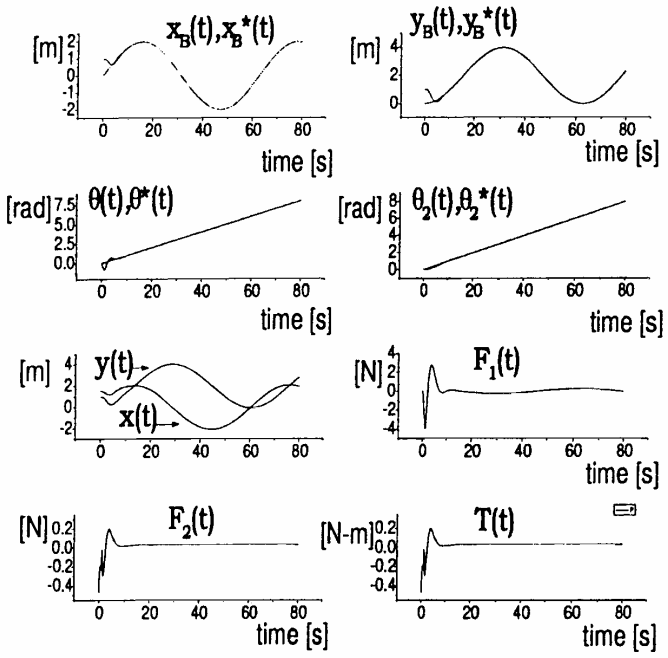

Figure 6: State variables, end effector position and control inputs responses for circle tracking maneuver with tangential arm pointing.

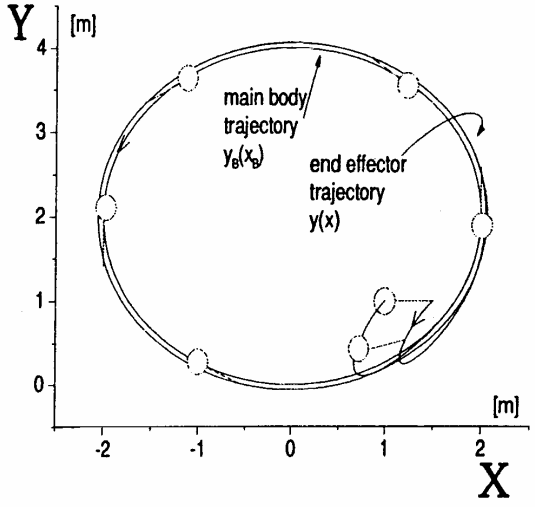

Figure 7: Circle tracking maneuver, main body and end effector position trajectories with tangential arm pointing.

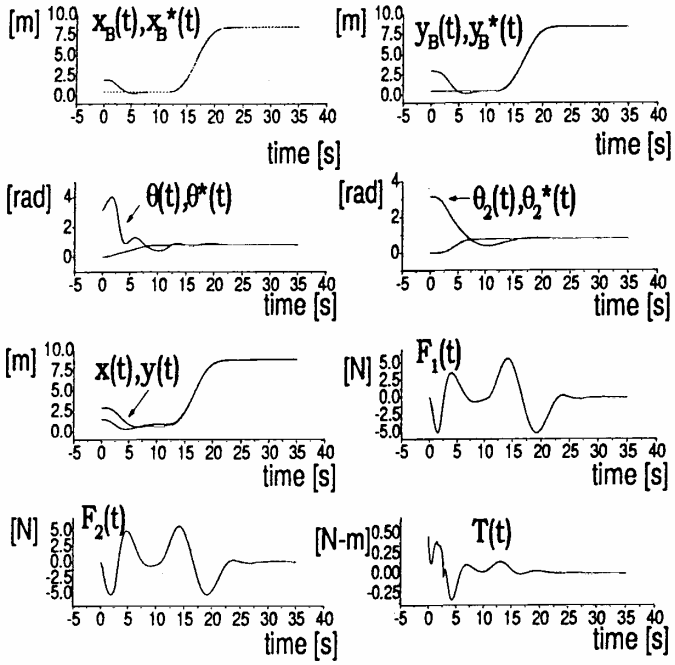

Figure 8: State variables, end effector position and control inputs responses for a rest to rest maneuver in a line segment.

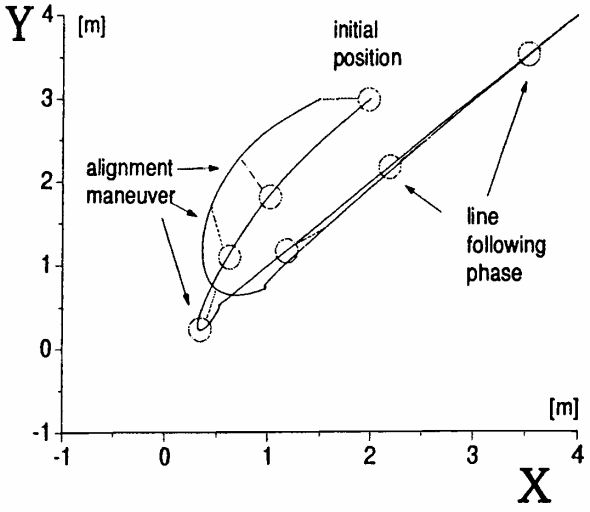

Figure 9: Portion of the line segment tracking maneuver: Main body and end effector position trajectories.